PCCP

Accepted Manuscript

ROYAL SOCIETY OF CHEMISTRY

www.rsc.org/pccp

Anatomy of Intramolecular Atomic Interactions in Halogen-Substituted Trinitromethanes

Ekaterina V. Bartashevich[1*], Ángel Martín Pendás[2] and Vladimir G. Tsirelson[3]
[1]*Department of Chemistry, South Ural State University (National Research University), 454080 Chelyabinsk, Russia, Phone: +7(351) 267-95-64, kbartash@yandex.ru*
[2]*Departamento de Química Física y Análitica, Facultad de Química, Universidad de Oviedo, 33006 Oviedo, Spain*
[3]*D.I. Mendeleev University of Chemical Technology, 125047 Moscow, Russia*

Abstract

The intramolecular interactions in substituted trinitromethanes, $XC(NO_2)_3$ (X = F, Cl, I, H) are studied and clarified by using a combination of the Quantum Theory of Atoms in Molecules (QTAIM), the Non-Covalent Interaction analysis and the Interacting Quantum Atoms (IQA) methods. The stretching vibration modes are formed by the concerted displacements of atoms involved in the covalent bonds showing the significant multiatomic influence in substituted trinitromethanes. In agreement with that, the arrangement of the local reduced density gradient minima indicates that the electron density favors the non-covalent intramolecular interactions X···O and N···O. However, the corresponding QTAIM bond paths are not formed; instead, such contacts, which we call *uncompleted links* in this context, are accompanied by "quasi-bonding channels" corresponding to $\lambda_2(\mathbf{r}) \leq 0$ regions on the sign$[\lambda_2(\mathbf{r})]\rho(\mathbf{r})$ contour maps. The intramolecular IQA energy contributions signal the appreciable electron exchange between the pairs of atoms associated with *potential atomic interactions* or the *bond-path-free* non-covalent links. The IQA analysis shows that the electrostatic term destabilizes $FC(NO_2)_3$ and distinctly stabilizes $IC(NO_2)_3$, it is close to neutral in $ClC(NO_2)_3$. The exchange energy between the X atom and the NO_2 groups, on the contrary, stabilizes all the molecules.

Keywords: halogenated trinitromethane compounds, non-covalent interactions, Interacting Quantum Atoms, NCI analysis, electron delocalization indices.

Introduction

Halogenated trinitromethane compounds (HTC) which are known as explosives and propellants are also of interest from the fundamental viewpoint[1-3]. Indeed, the specific structural organization of these compounds with an electronegative halogen and three nitro groups linked by a common carbon atom[4-6] leads to non-trivial mutual atomic influence. Unfortunately, the current interpretation of non-covalent intramolecular interactions in these systems may not seem satisfactory now. For example, the very short C−Cl covalent bond of 1.694(1) Å in chlorotrinitromethane crystal is explained as a result

of intramolecular electrostatic interactions between oppositely charged chlorine and oxygen atoms[7]. This explanation is based on the molecular electrostatic potential features and, therefore, is unable to span all the features of the atomic interactions. Therefore, it is of great interest to consider the nature of atomic interactions in HTC from the charge-density perspective. In the present study we focus on this point by using the Quantum Theory of Atoms in Molecules (QTAIM)[8], the Interacting Quantum Atom (IQA) method[9-12] and the NCI approach based on Reduced Density Gradient (RDG) analysis[13-15].

QTAIM[8] defines the boundaries of atoms in complex systems as the closed surfaces each containing only one nucleus; the flux of the gradient of electron density through these surfaces is zero. The bonding between atoms is associated with lines of maximal electron density, which link certain pairs of atomic basins, the bond paths. This association is based on observations[16,17], therefore the treatment of the bond paths as a necessary and sufficient sign of the *attractive* interatomic bonding, which accumulates influences of all the atoms in a system and finds their expression as the bridges of the electron density between specific atomic pairs[17], is in the focus of many studies[18-31]. They look at this problem from different viewpoints; however, the charge-density community is still far from the consensus in this question. For example, in an early application of the QTAIM to HCT, Cioslowski *et al.*[32,33] have already found three pairs of the bond paths and corresponding bond critical points (BCP) between oxygen atoms of the adjacent nitro groups[34] in $C(NO_2)_3^-$. They have noted[35,36], that the presence of bond paths delineate major interactions, which, however, do not have to be bonding. Indeed, they are not accompanied by any interaction energy value.

The IQA method[9,10] yields another approach to this problem. It provides an exact decomposition of the total molecular energy, E, into intra-atomic, $E_{self}(A)$, and interatomic, $E_{int}(A, B)$, components, which are computed by integration over one or two atomic basins, respectively, it is valid for both stationary and non-equilibrium geometries. In IQA, $E = \sum_A E_{self}(A) + \sum_{A<B} E_{int}(A, B)$, A, B label the atomic basins. $E_{self}(A)$ stands for the atomic self-energy, since it contains the kinetic energy of the electrons within the A atom, together with their electron-nucleus attraction to the A nucleus and their mutual electron-electron repulsion. If an atom is isolated, its self-energy is its total energy. Similarly, $E_{int}(A, B)$ contains all the energetic terms related to the pair of basins A, B: inter-basin nuclear repulsion, electron-nucleus attraction and electron-electron repulsion.

The usefulness of IQA is due to clear-cut separation of energetic scales: although total molecular energies are measured in thousands of kcal/mol, $E_{int}(A, B)$ is much smaller and easy to interpret chemically. To that end, it is useful to gather all the classical electrostatic terms contained in $E_{int}(A, B)$ (nuclear repulsion, electron-nucleus attraction, and the Coulomb part of the electron-electron repulsion) into the classical energy, $V_{clas}(A, B)$. This is the exact electrostatic interaction between the electrons and nuclei contained in atomic basins A and B. The remaining terms in $E_{int}(A, B)$ are purely quantum-mechanical in nature, depending only on the non-classical (exchange and correlation, $V_{xc}(A,$

B)) part of the electron-electron interaction. Summarily, $E_{int}(A, B) = V_{clas}(A, B) + V_{xc}(A, B)$. It has been shown[10-12] that $V_{clas}(A, B)$ measures the ionic-like component of a given interaction, while $V_{xc}(A, B)$ is linked to the electron-sharing or covalent-like energy contribution. Correspondingly, it may be used to locate the atomic pairs, which contribute to stabilization or destabilization of a system under consideration.

The atomic basins in IQA cannot be chosen unambiguously; however there are arguments that their determination according to the QTAIM is the most attractive[10,12]. Since the union of any set of QTAIM basins is also a zero-flux bounded region, the IQA analysis may be performed not only at the atomic level, but also at the functional group one. We will do that when we consider a nitro group in the following.

The NCI approach[13] is based on the analysis of the Reduced Density Gradient (RDG) distribution in intra- and intermolecular space. According to Ref.[13], low RDG regions are correlated to relevant interactions, either attractive (if $\text{sign}[\lambda_2(\mathbf{r})] <0$), or repulsive, if $\text{sign}[\lambda_2(\mathbf{r})] >0$. We note that any QTAIM critical point provides a null RDG, while the low RDG regions can be there where the critical points do not appear. Then the RDG analysis becomes a useful complementary tool for recognizing the uncompleted links as we will discuss below.

In the case of bond paths, their corresponding RDG region characterizes the presence of certain intermolecular interactions in both the calculated and experimentally electron densities[13-15, 37-39]. However, in the vicinity of ring and cage critical points, the treatment of low RDG regions is much vaguer. Moreover, the analysis of the electron density in perhalogenated ethanes $X_3C–CY_3$ (X, Y = F, Cl)[40] has revealed intramolecular RDG minima in the absence of any critical points in intramolecular regions of sterically hindered molecules.

It is worth noting that the nature of structure-forming non-covalent interactions between highly electronegative atoms located close to each other has always attracted much attention. The O···O bond paths in the dinitramide anions[41] and crystalline dinitrogen tetroxide[42] as well as the F···F ones in LiF[43] perfluorodiethyl ether[44], difluorinated aromatic compounds[45] and in orthorhombic chlorine trifluoride[46] have been determined. At the same time, association of the bond path between atoms which carry the same sign charge with a certain type of bonding − attractive or repulsive − does still remain a controversial issue.

The intramolecular X···O interactions (X = F, Cl, Br, and I) in a set of derivatives of 3-halopropenal with five-membered quasi-ring structures were investigated in [26,47]. Later the nature of the Cl···O contact in 3-chloropropenal was studied by using a dimer model[27]. The BCP parameters for these interactions allowed concluding that they had closed-shell nature as indicated by low values of electron density (0.008 − 0.013 a.u.) and positive values of both its Laplacian and the total electronic energy density. The authors[26] have concluded that all these X···O interactions are nonbonding and

destabilizing despite the bond path presence: that follows from the positive values of interaction energies obtained by several different methods. In the "open-closed method"[31,48] the energies of different conformers having exactly the same values of geometrical parameters as in the closed ZZ conformer are compared. The isodesmic reactions[49] method has also been used to that end. It has been shown[26,27] that the X···O interactions are characterized by negative values of MEP[50-52] both for halogen and oxygen, thus indicating electrostatic destabilization of a system.

The IQA energy partition for the same set of halogenated propenal derivatives with O···X intramolecular contacts (X = O, S, Hal) was discussed in [28]. As it turned out, the bond paths were not detected for all possible O···Hal interactions. It was concluded[28] that interatomic interaction energies did not serve as a universal tool for predicting the existence of bond paths between atoms. Another question concerns the nature of O···Hal intramolecular contacts: are the interactions between two electronegative atoms O···Hal stabilizing or destabilizing, and what factors define the nature of these interactions? The authors[28,29] have noted that the exchange energy is not predominant for the reported observations and that electrostatics usually establishes the sign of the total interaction energy between O and X. Nevertheless, the exchange energy could be used to predict the bond paths much better than the interaction energy.

The specificity of atomic interactions in HTC consists of the possible intramolecular indirect contacts between a connivent halogen atom and the X-facing oxygens of nitro groups in the absence of corresponding bond paths. As we will show below, the electron density in these areas tends to form the density "channels" along the interatomic vectors: they exhibit negative density curvatures $\lambda_1(\mathbf{r}) < 0$ and $\lambda_2(\mathbf{r}) < 0$ that are however not accompanied by a bond path. Such *bond-path-free* features can be considered as a signature of uncompleted links with low (but non-zero) RDG and negative $\lambda_2(\mathbf{r})$ values, and their characterization deserves a special attention. In this study we have examined these features of the electron density in the HTC molecules by combining QTAIM, RDG and IQA methods. We apply the QTAIM to locate the critical points and bond paths in electron density and to determine the atomic basins in HTC molecules. The RDG analysis has been applied to identify the possible non-covalent interactions. The quantitative evaluation of interatomic energy contributions has been done with the IQA approach; we used these contributions to establish their stabilizing or destabilizing influence on bonding between halogen and oxygen or nitrogen and oxygen of the neighboring nitro groups. It allowed us to get a deeper insight into the features of mentioned atomic interactions.

Theoretical Methods

The sample set of molecules $FC(NO_2)_3$ (**1**), $ClC(NO_2)_3$ (**2**), $IC(NO_2)_3$ (**3**), $HC(NO_2)_3$ (**4**), $ClC(CN)_3$ (**5**) has been used for analysis of intra-atomic non-covalent interactions. The computations of the wave functions have been carried out by the Kohn-Sham method[53] in the CPBE96/6-311G(d,p)

approximation[54,55] by applying the software package Firefly, version 8.0.0[56]. The functional CPBE96 includes 100% Hartree-Fock exchange and PBE correlation, and it leads to the shortening of C–Cl bond in the isolated molecule (1.677 Å).

Geometry optimizations have been carried out and the minimum-energy character of the equilibrium structures of all molecules has been confirmed by calculating their harmonic vibrational normal modes. CUBE-files for MEP and RDG functions have been prepared using the program Multiwfn 3.2.1[57]. The same program package has been used to construct the 2D contour maps of $\mathrm{sign}[\lambda_2(\mathbf{r})]\rho(\mathbf{r})$, the colored RDG($\mathbf{r}$) maps, and the RDG($\mathbf{r}$) – $\mathrm{sign}[\lambda_2(\mathbf{r})]\rho(\mathbf{r})$ diagrams for intra-molecular contacts. The 3D diagrams for RDG-indicated features have been obtained with the MoleCoolQt and MolIso programs[58,59].

The obtained wave functions have been used in further analysis of electron density. In particular, the electron density values $\rho(\mathbf{r}_b)$ and Laplacian of electron density $\nabla^2\rho(\mathbf{r}_b)$ at the bond critical points $\mathbf{r}_b$, of covalent bonds C–X and non-covalent contacts O···X, N···O (X = F, Cl, I, H) have been calculated. Electron Delocalization Indices $\delta(A, B)$[60,61] – the average number of electrons shared between the considered atoms A and B – have also been calculated. The QTAIM net atomic charges Q(A), have been obtained as differences between the nuclear charge of atom Z_A and integral electron population of corresponding atomic zero-flux basin. All the abovementioned descriptors have been calculated by AIMALL (version 13.10.19) software[62] and collected in the Table 1.

IQA analyses have also been performed with PROMOLDEN. Two words of caution should be said about the use of IQA-based partitioning in DFT calculations. When we use Kohn-Sham (KS) pseudo-wave functions, no true second-order density matrix is used; therefore, no well-defined electron-electron repulsion might be reached. IQA-DFT quantities, however, have been used successfully many times[28,63]. Also, at the single-determinant level, exchange-correlation energies are actually exchange-only contributions, $V_x(A, B)$.

Discussion

NCI analysis in the halogen-substituted trinitromethanes

The NCI approach based on the Reduced Density Gradient function reveals two types of low-valued spatial regions in the studied halogen-substituted trinitromethanes, described by C_{3v} symmetry, $XC(NO_2)_3$ – see Fig.1. First, three well-localized minima in RDG-indicated regions between the halogen atoms and each of three O atoms of nitro group are detected (contact X···O). Second, three minima in RDG-indicated regions between the N and O atoms for each pair of neighboring nitro groups are observed (contact N···O). Each RDG surface of 0.6 a.u. encompasses relatively high $\rho(\mathbf{r}) \leq 0.03$ a.u. electron density values for non-covalent interactions. The function $\mathrm{sign}[\lambda_2(\mathbf{r})]\rho(\mathbf{r})$[13] mapped onto the mentioned RDG-surface demonstrates that a significant part of each of the six surfaces,

inward-facing the molecule, lies in area of the positive values of $\lambda_2(\mathbf{r}) > 0$ (shown in red). The rest part on the periphery of RDG-surfaces lies in the range of negative values of $\lambda_2(\mathbf{r}) < 0$ (shown in blue). Green regions on the periphery of the RGD-surfaces with values $\lambda_2(\mathbf{r}) \approx 0$, correspond to very low values of the electron density $\rho(\mathbf{r}) \leq 0.006$ a.u. Note that, in contrast to halogenated molecules, only three RDG minima between atoms of N and O are observed in the trinitromethane.

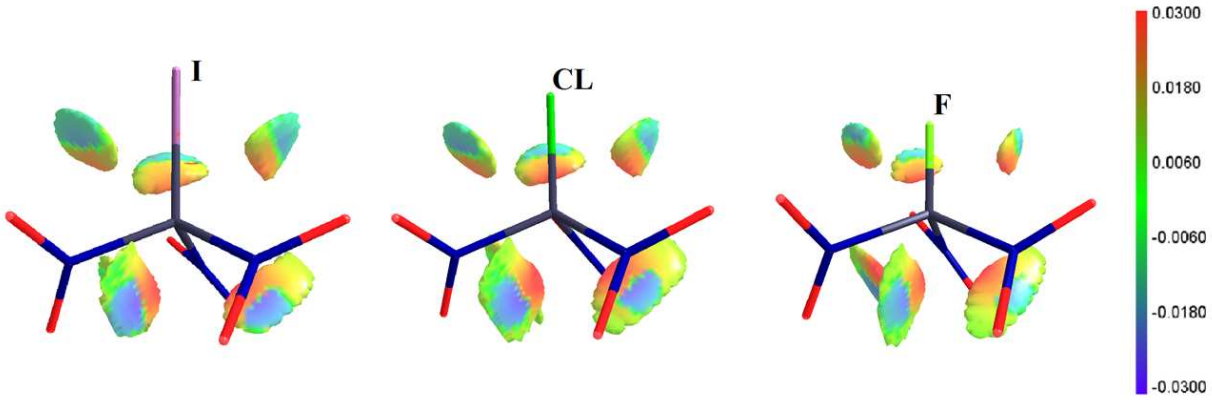

Fig.1. The RDG(**r**) isovalue in $HalC(NO_2)_3$ molecules and the mapped $sign[\lambda_2(\mathbf{r})]\rho(\mathbf{r})$ function

Let us now compare the RDG features in the $ClC(NO_2)_3$, $HC(NO_2)_3$ and $ClC(CN)_3$ with bonding information obtained by the other tools. In Figures 2–4, the molecular structures, the 2D $sign[\lambda_2(\mathbf{r})]\rho(\mathbf{r})$ contour maps, the colored RDG(**r**) maps and the RDG(**r**)–$sign[\lambda_2(\mathbf{r})]\rho(\mathbf{r})$ diagrams, as well as the superposition of these functions in significant planes, are presented. In this series the molecular symmetry is held, the Cl atom is replaced by an H atom, and the NO_2 group is replaced by a CN group. The RDG(**r**)–$sign[\lambda_2(\mathbf{r})]\rho(\mathbf{r})$ diagram for the $ClC(NO_2)_3$ (Fig. 2) shows the presence of two relatively wide spikes in the left part. They correspond to the two mentioned types of minima in RDG-indicated regions between Cl and O atoms and between O and N atoms belonging to neighboring nitro groups. In contrast, only one spike is detected in trinitromethane (Fig. 3); it corresponds to a decrease in the RDG between the nitro groups. And, finally, in $ClC(CN)_3$ (Fig. 4), where there is no steric hindrance created by the three nitro groups, and four electronegative substituents are present in halogenated trinitromethanes, there are no spikes on the RDG(**r**) – $sign[\lambda_2(\mathbf{r})]\rho(\mathbf{r})$ diagram associated with a decrease in the RDG.

The RDG(**r**) – $sign[\lambda_2(\mathbf{r})]\rho(\mathbf{r})$ plots together with $sign[\lambda_2(\mathbf{r})]$ colored density isolines show the RDG contact regions in the Cl-C-O and N-C-N planes in Fig. 2–4, where three interatomic boundaries corresponding to the condition of zero-flux of gradient of electron density[8] can also be seen. In the case shown in Fig. 2a, the interatomic boundaries of Cl and O atoms are coming extremely close; especially at the interatomic vector Cl···O, where they almost touch each other. However, the common boundary for Cl and O atomic basins is absent (Fig. 5) because the C and N atomic basins wedge between Cl and O atoms. Therefore, from the strict standpoint of the QTAIM theory, immediate pair-

wise atomic interactions Cl···O do not exist. Areas where four atomic basins meet each other are clearly revealed by the RDG function. The NCI-indicated region is placed between O and Cl atoms and the RDG function monotonically decreases in the orthogonal direction from the center to the periphery of the molecule. A similar situation takes place between O and N atoms belonging to neighboring nitro groups (Fig. 2b and 3): the O···N bond paths for atoms of neighboring nitro groups are not observed and four atomic basins form the local minima in NCI-indicated regions on the interatomic vector N···O in N-C-N-O fragment.

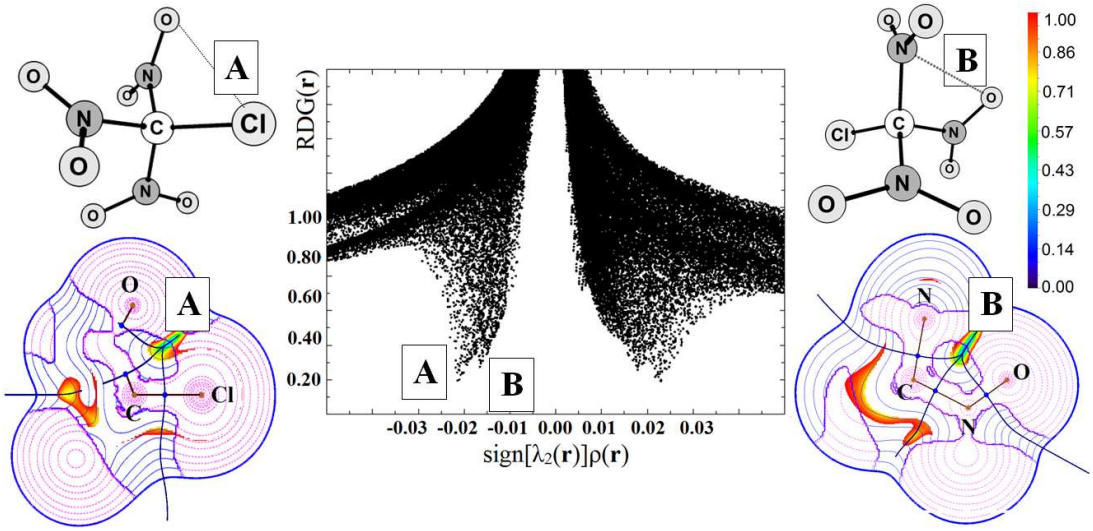

a b

Fig.2. Cl-C-O (a) and N-C-N (b) planes in $ClC(NO_2)_3$.

The contact regions are colored according to the RDG, to be read on the right scale. The contour lines of function sign[$\lambda_2(\mathbf{r})$]$\rho(\mathbf{r})$ are colored: blue lines correspond to $\lambda_2(\mathbf{r}) > 0$, while pink lines show $\lambda_2(\mathbf{r}) < 0$. Note that all the covalent bonds fall into the range of $\lambda_2(\mathbf{r}) < 0$. At the middle of Cl···O (A, left) and N···O (B, right) contacts, pink color regions with $\lambda_2(\mathbf{r}) < 0$ values are clearly seen.

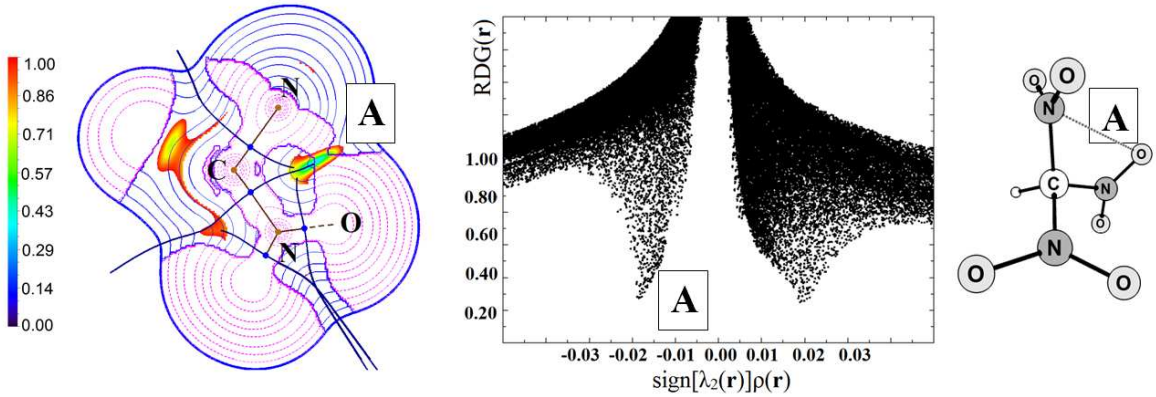

Fig.3. N-C-N plane in $HC(NO_2)_3$.

The RDG contact area between the N···O atoms is seen on the colored map. The contact regions are colored according to the RDG, to be read on the scale. There is no RDG minimum on the colored map between the H and O atoms, therefore only one spike is present on the RDG(**r**)–sign[λ_2(**r**)]ρ(**r**) diagram. The electron density is 0.019 a.u. at the RDG=0.25 minimum.

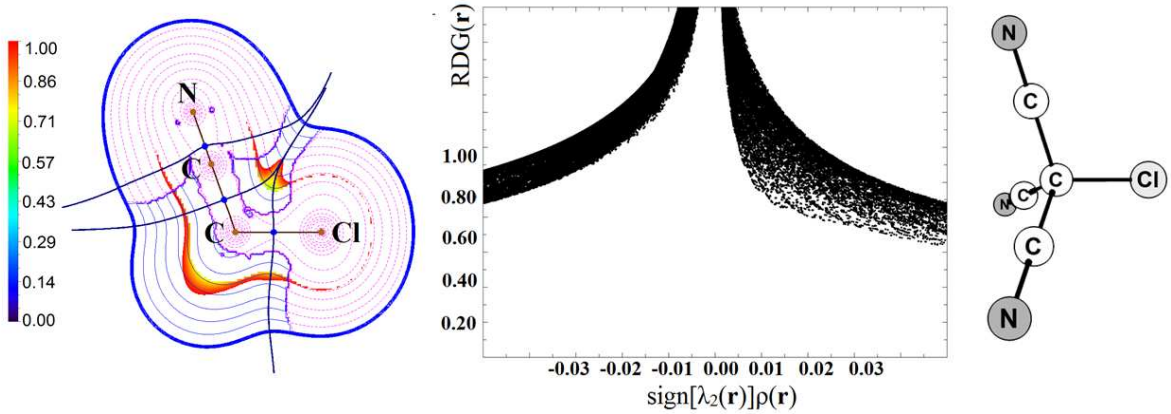

Fig.4. N-C-Cl plane in ClC(CN).

The contact regions are coloured according to the RDG, to be read on the scale. There are no significant RDG minima and corresponding spikes on the RDG(**r**)–sign[λ_2(**r**)]ρ(**r**) diagram for this intramolecular electron density organisation.

Let us consider the features of local regions defined by the sign of λ_2(**r**). The region with λ_2(**r**) ≤ 0 (shown by the pink-dotted lines in Fig. 2–4) always encloses the bond paths in the three-dimensional molecular space. Similar, the interatomic vectors Cl···O and N···O, despite the absence of corresponding bond paths, are enclosed by the volumes of negative values λ_2(**r**), each of such regions forms "channels" of electron density. Note that in the $ClC(CN)_3$ molecule (Fig. 4) the minimum of RDG between the Cl and N atoms is not observed and the "channels" in electron density and the regions with λ_2(**r**) ≤ 0 in the intramolecular space are absent. The interatomic surfaces in the N···O and Cl···O regions are extremely close and almost touch each other, but there is no direct contact between N and O or Cl and O.

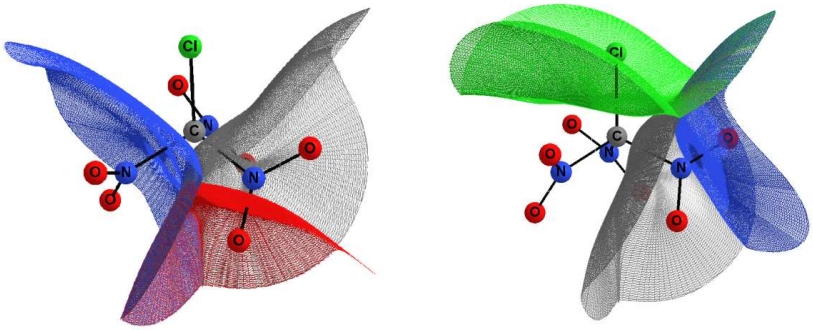

a) b)

Fig. 5. $ClC(NO_2)_3$: the interatomic surfaces in the a) N···O and b) Cl···O regions

According to the NCI viewpoint, the minima in the RDG-indicated regions around the corresponding interatomic vectors can be associated, in principle, with the presence of non-covalent interactions between the atoms or atomic groups in these regions. The existence of channels with $\lambda_2(\mathbf{r}) \leq 0$ between Cl···O and N···O atoms also supports the presence of corresponding atomic contacts, which are not accompanied by the formation of bond paths, however. As such channels are always observed for covalent bonds, we can speculate about their attractive nature. Further, the $\lambda_2(\mathbf{r})$ function changes its sign close to the Cl···O and N···O vectors; that adds to the idea that interactions in the studied structural fragment are not described as the sum of the pair-wise atom-atom interactions only: the electron-density curvature in this fragment is formed by contributions of several atoms and directly affects the nature of the atomic interactions in the abovementioned intramolecular regions. It looks as if the RDG approach would indicate a variety of areas which are or can be associated with *potential* atomic interactions (uncompleted links), pair-wise or multiple (many-atomic) contacts, while the bond paths of QTAIM identifies the immediate pair-wise atomic interactions among them.

Atom-atom interaction properties: IQA energies and delocalization indices

The calculated IR stretching vibration frequency of C–Cl bond (B3PW91/6-31G(d,p)) in methyl chloride (743.9 cm^{-1}) and chlorotrinitromethane (1041.8 cm^{-1}; d(C–Cl) = 1.713 Å)[7] showed that trinitromethyl group caused a significant frequency increasing (300 cm^{-1}), the so-called blue shift. This fact signaled about C–Cl bond length shortening in the gas phase. Calculation for the chlorotrinitromethane dimer with halogen bond O···Cl showed that dimerization had almost no influence on the frequency and Cl–C bond length[7].

Our computation has shown that C–Cl mode in $ClC(NO_2)_3$ with frequency of 1020.3 cm^{-1} (an intensity is 1.06 km/mol) corresponds to complex vibration: extension of the C–Cl bond is accompanied by a decrease of the C–N bond distance. Also, the N=O bonds of all nitro groups also take part in the formation of this vibration. Restoring the displacement of atoms along vibration modes

on the same scale shows that the shortening of the C–N stretching vibration amplitude is about 80% of the elongation of C–Cl bond. The next vibration containing a large contribution of C–Cl bond has a frequency of 1263.4 cm^{-1} (with an intensity of 2.30 km/mol). Contribution of C–N bond to this mode is about 50% according to the ratio of amplitudes. It can be noted that there are two constituent vibrations – 798.9 cm^{-1} and 510.9 cm^{-1} – involving the C–Cl bond stretching. However, they show very low intensities: 0.25 and 0.02 km/mol, correspondingly. Vibrations for the light F atom more favorably admix with the vibrations of nitro groups. In general, the complex stretching vibrations, when the simultaneous displacements of atoms involved to the bonds C–X, C–N and N=O, are observed, it indicates the large multiatomic nature of these interactions in halogenated trinitromethanes.

According to the early experimental investigations of reactivity and chemical properties of halotrinitroalkanes[64], the strength of C–X interaction increases as C–I < C–Br < C–Cl < C–F. Redox process at the dropping mercury electrode for these compounds also gives a similar series: the bond strength C–X grows from I to Cl because of reduced positive half-wave potential values $E_{1/2}$[64] from iodine to chlorine. In general, the C–X bonds in substituted trinitromethanes are essentially less strong than bonds in haloalkanes. It is assumed that after dissociation of the C–X bond, the halogen leaves a molecule with notable deficiency of electrons that likely has a positive charge. This hypothesis is confirmed by the oxidative power of the eliminated halogen: it oxidizes hydrazine into molecular nitrogen[64]. In halotrinitromethanes, calculated delocalization indices[60,61] for C–X bonds (Table 1) are inversely correlated to the experimentally observed strength of these bonds. The bond C–F has the lowest delocalization index δ(C–F) = 0.67; the highest delocalization index is δ(C–Cl) = 1.1, and δ(C–I) = 1.04 is just slightly lower. Note that the delocalization indices for C–N bonds vary significantly from 0.58 to 0.76, while for N···O contact δ = 0.050 ± 0.004 remains nearly constant. The inverse relationship between δ and the bond strength can be explained by the fact that δ reflects the electron delocalization, which arises from the covalent fraction of bonding[60]. However, in practice it is often the heterolytic (ionic) mechanism for the C–X bond dissociation which is observed in such systems[64]. On the other hand, it is interesting to observe how the delocalization indices, being characteristic of atom-atom interactions, allow interpreting the nature of the intramolecular interactions Cl···O and N···O involving significant influence of other distant atoms.

Table 1. Electron density, $\rho(\mathbf{r}_b)$, and Laplacian of electron density, $\nabla^2\rho(\mathbf{r}_b)$ at the bond critical points together with electron delocalization indices, δ(A, B), and IQA energy contributions (kcal/mol) for atomic contacts in substituted trinitromethanes

Molecule	Bond/ Contact	$\rho(\mathbf{r}_b)$, a.u	$\nabla^2\rho(\mathbf{r}_b)$, a.u	δ(A, B)	V_{clas}	V_x	E_{int}
$HC(NO_2)_3$	C – H	0.306	-1.231	0.832	84.7	-164.8	-80.1
	C – N	0.286	-0.978	0.739	33.3	-154.1	-120.7

	H···O	–	–	0.014	-15.5	-1.4	-16.9
	H···O'	–	–	0.009	-11.7	-0.5	-12.2
	H···N	–	–	0.031	11.9	-3.5	8.4
	O···N	–	–	0.046	-32.2	-5.8	-37.9
$FC(NO_2)_3$	C – F	0.321	0.691	0.668	-477.4	-141.7	-619.1
	C – N	0.298	-1.060	0.697	127.9	-151.3	-23.4
	F···O	–	–	0.054	46.1	-6.3	39.8
	F···O'	–	–	0.015	34.0	-0.9	33.2
	F···N	–	–	0.098	-49.7	-12.5	-62.2
	O···N	–	–	0.046	-36.7	-6.0	-42.7
$ClC(NO_2)_3$	C – Cl*	0.247 0.246	-0.533 -0.521	1.103 1.105	45.8 45.4	-198.4 -198.7	-152.5 -153.3
	C – N	0.287 0.286	-0.968 -0.957	0.742 0.742	82.9 84.3	-157.5 -157.3	-74.5 -72.9
	Cl···O	–	–	0.073 0.073	-0.7 -0.02	-7.7 -7.7	-8.4 -7.7
	Cl···O'	–	–	0.019 0.019	-2.1 -1.4	-0.9 -0.9	-3.0 -2.3
	Cl···N	–	–	0.078 0.076	0.6 0.8	-7.4 -7.4	-6.8 -6.5
	O···N	–	–	0.051 0.051	-39.5 -39.9	-6.9 -6.8	-46.4 -46.7
$IC(NO_2)_3$	C – I	0.131	0.137	1.037	31.0	-149.9	-119.0
	C – N	0.284	-0.958	0.761	45.7	-154.4	-113.7
	I···O	–	–	0.078	-30.8	-7.5	-38.3
	I···O'	–	–	0.019	-23.3	-0.8	-24.1
	I···N	–	–	0.060	31.8	-4.8	27.0
	O···N	–	–	0.052	-38.3	-7.0	-45.4
$ClC(CN)_3$	C – Cl	0.213	-0.396	1.051	19.3	-178.8	-159.5
	Cl···C	–	–	0.087	-3.9	-8.4	-12.4
	Cl···N	–	–	0.045	7.0	-2.5	4.6

*For $ClC(NO_2)_3$ molecule different calculation data are offered: CPBE96/6-311G(d,p) in the first line, CPBE96/6-311+G(d,p) in the second line

The delocalization indexes which are built on Kohn-Sham orbitals must be taken cautiously since they do not include the electron correlation effect[65]. IQA[66] energy decomposition analysis allows better ascertaining the nature of the intramolecular interactions in the $XC(NO_2)_3$ (X = F, Cl, I, H) molecules. Classical (Coulomb), exchange, and total energy components for most of the relevant interactions are shown in Table 1. The first interesting point regards the C–X interaction. Its covalent or exchange energy component, V_x, roughly follows the values of $\delta/R_{C\text{-}X}$, as already noticed[67], evolving from –141 kcal/mol in the $FC(NO_2)_3$ to –198, –150, and –165 kcal/mol in the rest of the series, respectively. This allows for an easy rationalization of the covalent contributions to C–X bonds.

The electrostatic or ionic energy component, V_{clas}, is purely classical in nature, and it is usually dominated by the monopolar terms, $Q_C Q_X/R_{C\text{-}X}$, together with generally smaller dipolar energies. This simple fact also explains the sequence that we have found, which in the above order, is –477.4, +45.8, +31.0, and +84.7 kcal/mol. Notice that the energy of the C–F interaction has a considerably larger V_{clas} than V_x component, and that the rather large increase of V_{clas} when we pass from X = I to X = H is related to the drop in the C–X bond distance. Adding the V_{clas} and V_x terms together, the C–X interaction energies turn out to be –619.1, –152.5, –119.0, and –80.1 kcal/mol.

If we restrict ourselves to the halogen-substituted compounds, these facts allow us to understand the origin of the failure of δ in these systems, the value which has been successfully used to measure bond strengths: the electrostatic contribution to bonding cannot be neglected in very polar interactions. Bonding is usually dominated by the V_x terms, since the different V_{clas} contributions tend to cancel out: if there is an appreciable electron transfer from atom A to atom B, for instance, the electrostatic stabilization achieved through the dominant $Q_A Q_B/R$ term will be balanced by the (large) destabilization in E_{self}(A), which may be estimated as a product of Q_A and IP(A), where IP(A) is the ionization potential of A. However in cases such as the ones that we are examining, the large electrostatic terms alter the conclusions drawn from δ or V_x, and their consideration is essential to understand the bond strength.

It is also interesting to analyze the C–N interaction. Given its relatively constant distance, the δ(C–N) value correlates well with the covalent C–N energy contribution V_x (C, N), which is –151, –158, –159, and –154 kcal/mol for the X = F, Cl, I, H series. The electrostatic contribution is always destabilizing, due to the relatively high positive charges of C and N in all cases, and according to the previous arguments, it markedly decreases on passing from fluorine to iodine to hydrogen. In the end, the C–N interaction energy evolves along the following sequence; –23.4, –74.5, –113.8, –120.7 kcal/mol.

Let us now turn to consideration of the relevant halogen indirect contacts X···O, where O is the X-facing oxygen of a NO_2 group. It is found that the electrostatic energy contribution depends on the sign of the X atomic charge. It changes from +40 kcal/mol when X = F to –38 kcal/mol when X = I. More interesting is the change in energy of its corresponding (through-space) electron-sharing (covalent, exchange) terms V_x(X···O): –6.3, –7.7, –7.5, –1.4 kcal/mol along the series. Also remarkable are the V_x(X···N) values: –12.5, –7.4, –4.8, –3.5 kcal/mol, respectively. The V_x(X···O') terms, where O' is the X-opposing oxygen of the nitro groups, are considerably smaller. Notice how the trinitromethane molecule has very small X···H exchange. This is clearly compatible with the absence of an RDG spike in the $HC(NO_2)_3$ RDG plot commented above. Adding together the X···N and X···O exchange interactions, and taking into account that there are three equivalent nitro groups, we get, for instance, that the energy V_x stabilizes the $XC(NO_2)_3$ molecules by about 59, 48, 39, and 16

kcal/mol along the X = F, Cl, I, H series. For the halogens these are values that cannot be considered negligible in respect to the V_x(C, X) or E_{int}(C, X) energies. This is an important actor in the explanation of the short C–X distances found in the halogen-substituted trinitromethanes.

The IQA energy for O···N contacts has led us to two important observations about the ranking of stabilizing interactions in substituted trinitromethanes. First, O···N interactions are stabilized due to electrostatic component V_{clas} (see Table 1). The stabilization effect through the three nitro groups per $ClC(NO_2)_3$ molecule is –139.2 kcal/mol. It is comparable with energy of the covalent C–Cl bond: –152.5 kcal/mol. The same stabilization energy exceeds the energy of the C–I covalent bond in $IC(NO_2)_3$ by 17.2 kcal/mol, and the energy of the C–H covalent bond in $HC(NO_2)_3$ molecule by 33.6 kcal/mol. Second, it has become clear how the variation of the X atom (X = F, Cl, I, H) leads to a change in priority among the pair-atomic contributions to the stabilization of the whole system. In the $IC(NO_2)_3$ molecule, the stabilizing contributions through the nitro groups, I···O interactions and covalent bond C–I are equally distributed. Contributions of the C–N covalent bonds are large in all these molecules. In $HC(NO_2)_3$, the stabilization through the three nitro groups exceeds that through the covalent bond C–H. In the $ClC(NO_2)_3$ molecule, the covalent bond C–Cl dominates in the stabilization of the whole system. This fact is also in good agreement with the "abnormally" short C–Cl bond distance in chlorotrinitromethane[7].

The comparison of V_x(X···N) and V_x(X···O) is also interesting. It favors the X···N contribution in $FC(NO_2)_3$ (–12.5 and –6.3 kcal/mol, correspondingly), and shifts progressively towards favoring the X···O contact as the halogen grows in size (–4.8 and –7.5 kcal/mol in $IC(NO_2)_3$). Notice that there is no accordance in the identification of the possible X···N, X···O and N···O interactions by V_x and NCI. NCI -indicated regions are present between X and O atoms and between O and N atoms being far from the X···N vector. At the same time, values V_x(Cl···O) = –7.4 and V_x(Cl···N)= –7.7 kcal/mol are very close to each other in $ClC(NO_2)_3$.

IQA methodology represents that the estimation of the exchange V_x(A, B) and electrostatic V_{clas}(A, B) components of interacting atoms energies is suitable for predicting the bond path existence[28,29] between the atoms. Comparing the interaction between electronegative atoms O···Cl in the series of substituted propenal, the authors[28,29] noticed that the electrostatically destabilizing interactions ($V_{clas} > 0$) could not be compensated by a contribution of the exchange energy V_x. In work[28] the numerical criterion $\alpha = V_x/V_{clas}$ ($-1 < \alpha < 0$ for positive V_{clas} values) has been suggested. Our α values support this observation: $\alpha = -0.13$ for F···O and $\alpha = -0.43$ for Cl···O interactions.

Similarly, the Ref.[28,29] appointed that the value $\beta = V_x^{primary}/ V_x^{secondary}$ seemed an appealing numerical criterion: the "primary" interactions were accompanied with the bond path while the "secondary" ones were not. We have checked this statement for the systems with multiple interactions O···X, N···X (X = H, F, Cl, I). In substituted trinitromethane molecules, the bond paths are absent in

all cases of non-covalent interactions O···X, N···X. We have verified that despite the relatively close exchange energy contributions, the interactions F···O and I···O essentially differ in the electrostatic stabilization. It is interesting that the electrostatic components V_{clas} of O···X, N···X interactions tend to compensate each other in all molecules examined here. Note that in the molecule $FC(NO_2)_3$ the electrostatic stabilization ($V_{clas} < 0$) is entered by the interaction between halogen and nitrogen atoms, as compared with the molecule $IC(NO_2)_3$, where the stabilization appears between halogen and oxygen. This fact is clearly illustrated in Fig. 6. The values V_x and V_{clas} of O···Cl and N···Cl interactions are very small, but they are mutually compensated in the $ClC(NO_2)_3$ molecule. Thus, generally speaking, it is impossible to give priority in stabilizing mission to N···X or O···X interactions in substituted halotrinitromethanes. A halogen atom directly defines which interaction (with N or with O) will be electrostatically stabilizing in $XC(NO_2)_3$ molecules.

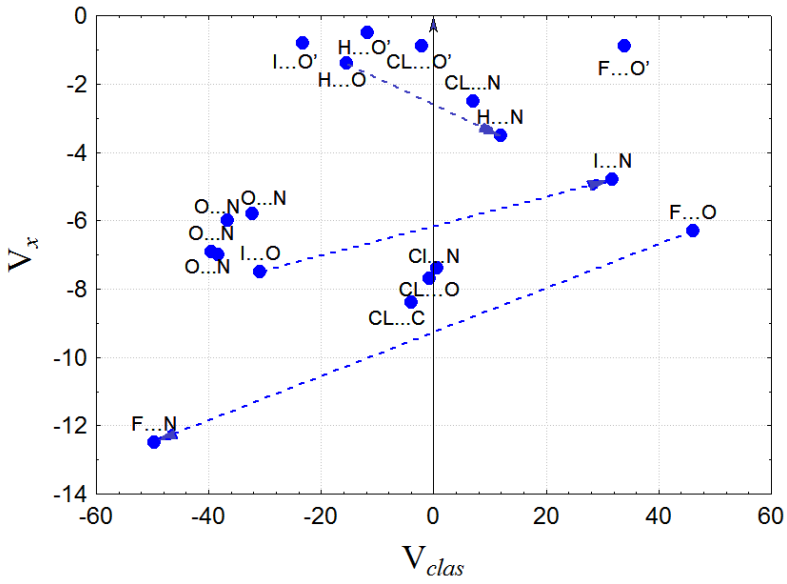

Fig. 6. Exchange and electrostatic IQA energy contributions (kcal/mol) for atomic interactions in substituted trinitromethanes and $ClC(CN)_3$ molecule

The numerical ratios $V_x(O\cdots X)/V_x(N\cdots X)$ decrease in our molecule series from I to H (I > Cl >F > H) as 1.7, 1.0, 0.5, 0.4. The ratio $V_x(O\cdots Cl)/V_x(N\cdots Cl)$ is lower than β-criterion from Ref[28] (β = 1.35 for O···Cl interaction). This condition is completely consistent with our observations: between chlorine and oxygen in the $ClC(NO_2)_3$ molecule the bond path should not exist.

We also like to show in the quantitative manner that electrostatics alone, as stated in Ref[7], cannot be responsible for shortening the X–C bond distance. The V_{clas} values provided by IQA measure exactly the classical electrostatic interaction among all the electrons and nuclei contained in two different regions of the space, for example, in the X and C atomic basins. They thus include full volumetric density reorganizations that accompany the formation of a bond of or an interaction, and

not only those that can be visually grasped from examining the value of the MEP in more or less arbitrarily chosen around-molecule electron-density surfaces. We conclude that the sign of electrostatic interactions cannot (and should not) be obtained from the surface-mapped MEP values.

This is particularly clear in the examples considered in this study: the V_{clas} energy series examined in the previous paragraph shows that X···O electrostatic interactions evolve in the opposite direction expected from surface mapping. The V_{clas} would destabilize the $FC(NO_2)_3$ compound, would be neutral in the $ClC(NO_2)_3$ molecule, and would heavily stabilize the $IC(NO_2)_3$ and $HC(NO_2)_3$ systems. If the complete nitro group is taken into account instead, the situation stays the same: the V_{clas} (X···NO_2) values are +30.0, –2.3, –22.3, and –15.3 kcal/mol along the series. Actually, V_{clas}(X···NO_2) is almost fully determined by the V_{clas}(X···O') values: +34.0, –2.1, –23.3, and –11.7 kcal/mol, where O' is the more distant oxygen atom from X in a nitro group. This means that the electrostatic interaction between the X atom and the N and O atoms almost cancel each other. It is not V_{clas}, but V_x that correlates with the C–X bond length shortening that is found for X = halogen (and absent when X = H). More indications pointing towards this view are easily found. For instance, the O (X facing oxygen) net charge is rather insensitive to the system, but shows a very smooth variation, –0.497, –0.509, –0.519, –0.524 e. It is known[67] that electronic charge flows to maximize stabilization by electrostatic terms in similar molecules, so if electrostatics is behind the short X–C distances in these systems, the negative charge on O atom should decrease in the above sequence. In fact, the numbers above show that the electrons in the O atom avoid the region facing towards negatively charged species like the F atom, as much as possible, and flow towards positively charged ones, like the H atom.

Conclusion

Combined QTAIM and NCI analysis of electron density has led us to the following picture of the atomic interactions in substituted trinitromethanes, $XC(NO_2)_3$ (X = F, Cl, I, H). The NCI approach exhibits six regions in each molecule (three in the $HC(NO_2)_3$), which, in principle, favors the formation of intramolecular interactions X···O (X = F, Cl, I) between a halogen and the nearest X-facing oxygen atom as well as between the three nitro groups along the N···O line. However, corresponding bond paths in electron density are not found. The comprehensive anatomy of electron density features in substituted trinitromethanes is revealed by different tools compatible among each other, and has led us to define the uncompleted *bond-path free* non-covalent intramolecular interactions X···O (X = F, Cl, I) and N···O in multicenter structural fragments. The last assertion is in conformity with harmonic IR frequency analysis that has shown that the stretching vibration modes are formed by the concerted displacements of atoms involved in the covalent bonds. At that, the neighboring carbon and nitrogen atomic basins penetrate into the interatomic space as extremely thin layers preventing possible direct

N···O and X···O contacts. For such contacts, we observe low RDG quasi-bonding channels embracing the electron density values with $\lambda_1(\mathbf{r})<0$ and $\lambda_2(\mathbf{r})<0$ that extended in a space between oxygen, nitrogen and halogen, rather than bond paths. These channels correspond to $\lambda_2(\mathbf{r}) < 0$ regions on the two-dimensional sign$[\lambda_2(\mathbf{r})]\rho(\mathbf{r})$ contour maps.

The IQA method, which allows estimating the diatomic contributions to the total molecular energy irrespective of presence/absence of corresponding bond paths, enabled us to compute the corresponding energy values for both covalent bonds (C–X, C–N) and non-covalent contacts (X···O, N···O) in our set of halogenated molecules. The energy of corresponding through-space exchange terms V_x(X···O) has the lowest negative value for X = Cl and the highest value for X = H. For the latter case it becomes clear that the absence of an RDG spike is a result of very low H···O exchange in the $HC(NO_2)_3$. In this sense IQA has also shown to be compatible with the basic RDG results.

Considering the multiple *bond-path-free* non-covalent contacts as *interactions* of a halogen with three equivalent nitro-groups, we have found that the corresponding exchange energy V_x stabilizes the F-, Cl-, and I-trinitromethanes by 59, 48, and 39 kcal/mol, respectively. These data explain the short C–Cl bond length of 1.694(1) Å found in chlorotrinitromethane[7]. IQA calculations show that the classical electrostatic interaction among all the electrons and nuclei contained in the space between halogen and entire nitro group would destabilize the $FC(NO_2)_3$ compound, would be neutral in the $ClC(NO_2)_3$ molecule, and would heavily stabilize the $IC(NO_2)_3$ system. Thus, the combinations of different approaches has enabled us to reach a deeper insight into the nature of complicated and even uncompleted links where the application of the standard QTAIM does not find fully developed bond critical points.

Acknowledgments

This work was supported by the Russian Foundation for Basic Research, grant 13-03-00767a and grant 14-03-00961a. Financial support from the Spanish Government, grant CTQ2012-31174 is also acknowledged.

References

1. Politzer, P.; Murray J. S. *Energetic Materials. Part 2. Detonation, Combustion* in *Theoretical and Computational Chemistry,* Elsevier, Amsterdam, **2003**, 474.
2. Rice, B. M.; Byrd, E. F. C.; Mattson W. D. *Computational Aspects of Nitrogen-Rich HEDMs* in *High Density Materials, Vol. 125* (Eds.: T. M. Klapötke), **2007**, 153–194.
3. Göbel, M. *Energetic Materials Containing The Trinitromethyl Pseudohalide Functionality.* Dissertation, Der Ludwig-Maximilians-Universität München, **2009**, 410.
4. Will, W. *Hexanitroethane*. *Chem. Ber*. **1914,** *47*, 961–965.

5. Levchenkov, D. V.; Kharitonkin, A. B.; Shlyapochnikov, V. A. *Molecular structures of trinitromethane derivatives. Russ. Chem. Bull.* **2001**, *50*, 385–389.
6. Shlyapochnikov, V. A.; Fainzil'berg, A. A.; Novikov, S. S. *The spectra and structures of halogen derivatives of trinitromethane. Izv. Akad. Nauk SSSR* **1961**, *3*, 519–520.
7. Göbel, M. Tchitchanov, B. H. Murray, J. S.; Politzer, P. Klapotke, T. M. *Chlorotrinitromethane and its exceptionally short carbon–chlorine bond.* Nature Chemistry, **2009**, *1*, 229–235.
8. Bader, R. F. W. *Atoms in Molecules. A Quantum Theory.* Oxford University Press, New York, **1990**, 438.
9. Martín Pendás, A.; Blanco, M. A.; Francisco, E. *Two-electron integrations in the quantum theory of atoms in molecules. J. Chem. Phys.* **2004,** *120*, 4581–4592.
10. Blanco, M. A.; Martín Pendás, A.; Francisco, E. *Interacting Quantum Atoms: A Correlated Energy Decomposition Scheme Based on the Quantum Theory of Atoms in Molecules. Chem. Theory Comput.* **2005**, 1, 1096–1109.
11. Martín Pendás, A.; Blanco, M. A.; Francisco, E. *A Molecular Energy Decomposition Scheme for Atoms in Molecules. J. Chem. Theory Comput.* **2006,** *2*, 90–102.
12. Martín Pendás, A., Blanco, M. A.; Francisco, E. J. *Chemical Fragments in Real Space: Definitions, Properties, and Energetic Decompositions*. *J. Comput. Chem.* **2007,** *28*, 161–184.
13. Johnson, E. R.; Keinan, S.; Mori-Sanchez, P.; Contreras-Garcia, J.; Cohen, A. J.; Yang, W. *Revealing Noncovalent Interactions*. *J. Am. Chem. Soc.*, **2010**, *132*, 6498–6506.
14. Contreras-Garcia, J.; Johnson, E. R., Keinan, S., Chaudret, R.; Piquemal, J.-P.; Beratan, D. N.; Yang, W. *NCIPLOT: A Program for Plotting Noncovalent Interaction Regions. J. Chem. Theory Comput.*, **2011**, *7*, 625–632.
15. Otero-de-la-Roza, A.; Johnson, E. R.; Contreras-Garcia, J. *Revealing non-covalent interactions in solids: NCI plots revisited. Phys. Chem. Chem. Phys.* **2012***, 14*, 12165–12172.
16. Runtz, G. R.; Bader, R. F.W.; Messer, R.R. *Definition of bond paths and bond directions in terms of the molecular charge distribution. Can. J. Chem.* 1977, *55*, 3040–3045.
17. Bader, R. F. W. *A Bond Path: A Universal Indicator of Bonded Interactions*. *J. Phys. Chem. A* **1998**, *102*, 7314−7323.
18. Tsirelson, V. G. *The measurement and use of topological features of the experimental electron density. Acta Cryst. A* 52 Suppl., **1996**, C-554.
19. Haaland, A.; Shorokhov, D. J.; Tverdova, N. V. *Topological Analysis of Electron Densities: Is the Presence of an Atomic Interaction Line in Equilibrium Geometry a Sufficient Condition for the Existence of a Chemical Bond? Chem.- Eur. J.* **2004**, *10*, 4416−4421.
20. Poater, J.; Solà, M.; Bickelhaupt, F. M. *Hydrogen-Hydrogen Bonding in Planar Biphenyl, Predicted by Atoms-In-Molecules Theory, Does Not Exist. Chem.-Eur. J.* **2006**, *12*, 2889−2895.

21. Martín Pendás, A.; Francisco, E.; Blanco, M. A.; Gatti, C. *Bond Paths as Privileged Exchange Channels. Chem.-Eur. J.* **2007**, *13*, 9362−9371.
22. Bader, R. F. W. *Bond Paths Are Not Chemical Bonds. J. Phys. Chem. A* **2009**, *113*, 10393−10396.
23. Grimme, S.; Mück-Lichtenfeld, C.; Erker, G.; Kehr, G.; Wang, H.; Beckers, H.; Willner, H. *When Do Interacting Atoms Form a Chemical Bond? Spectroscopic Measurements and Theoretical Analyses of Dideuteriophenanthrene. Angew. Chem., Int. Ed.* **2009**, *48*, 2592−2595.
24. Bader, R. F. W. *Definition of Molecular Structure: By Choice or by Appeal to Observation? J. Phys. Chem. A* **2010**, *114*, 7431−7444.
25. Dem'yanov, P.; Polestshuk, P. *A Bond Path and an Attractive Ehrenfest Force Do Not Necessarily Indicate Bonding Interactions: Case Study on M2X2 (M = Li, Na, K; X = H, OH, F, Cl). Chem.-Eur. J.* **2012**, *18*, 4982−4993.
26. Jabłoński, M. *Energetic and Geometrical Evidence of Nonbonding Character of Some Intramolecular Halogen···Oxygen and Other Y···Y Interactions. J. Phys. Chem. A* **2012**, *116*, 3753−3764.
27. Jabłoński, M.; Palusiak, M. *The halogen···oxygen interaction in 3-halogenopropenal revisited − The dimer model vs. QTAIM indications. Chem. Phys.* **2013**, *415*, 207−213.
28. Tognetti, V.; Joubert, L. *On the physical role of exchange in the formation of an intramolecular bond path between two electronegative atoms. J. Chem. Phys.* **2013**, *138*, 24102−24109, and references therein.
29. Tognetti, V.; Joubert, L. *On critical points and exchange-related properties of intramolecular bonds between two electronegative atoms. Chem. Phys. Lett.* **2013,** *579*, 122–126.
30. Syzgantseva, O. A. Tognetti, V.; Joubert, L. *On the Physical Nature of Halogen Bonds: A QTAIM Study. J. Phys. Chem. A*, **2013**, *117* (36), 8969–8980.
31. Jabłoński, M.; Monaco, G. *Different Zeroes of Interaction Energies As the Cause of Opposite Results on the Stabilizing Nature of C−H···O Intramolecular Interactions. J. Chem. Inf. Model.* **2013**, *53*, 1661−1675.
32. Mixon, S. T.; Cioslowski, J. *Covalent vs Ionic Bonding in Hexasubstituted "Push-Pull" Ethanes. J. Am. Chem. Soc.* **1991**, 113, 6766−6771.
33. Cioslowski, J.; Mixon, S. T.; Fleischmann, E. D. *Electronic Structures of Trifluoro-, Tricyano-, and Trinitromethane and Their Conjugate Bases. J. Am. Chem. Soc.* **1991**, *113*, 4755–4761.
34. Cioslowski, J.; Mixon, S. T.; Edwards, W. D. *Edwards, Weak Bonds in the Topological Theory of Atoms in Molecules. J. Am. Chem. Soc.* **1991**, *113*, 1083–1085.

35. Cioslowski, J.; Mixon, S. T. *Topological properties of electron density in search of steric interactions in molecules: electronic structure calculations on ortho-substituted biphenyls*. *J. Am. Chem. Soc.* **1992,** 114, 4382–4387.

36. Cioslowski, J.; Edgington, L.; Stefanov, B. B. *Steric Overcrowding in Perhalogenated Cyclohexanes, Dodecahedranes, and [60]Fulleranes J. Am. Chem. Soc.* **1995**, 117, 10381–10384.

37. Saleh, G.; Gatti, C.; Presti, L. L.; Contreras-Garcia. *Revealing Non-covalent Interactions in Molecular Crystals through Their Experimental Electron Densities*. J. *Chem. Eur. J.*, **2012,** *18*, 15523–15536.

38. Johnson, E. R.; Otero-de-la-Roza, A. *Adsorption of Organic Molecules on Kaolinite from the Exchange-Hole Dipole Moment Dispersion Model. J. Chem. Theory Comput.*, **2012**, *8*, 5124–5131.

39. Saleh, G.; Presti, L. L.; Gatti, C.; Ceresoli, D. *NCImilano: an electron-density-based code for the study of noncovalent interactions*. *J. Appl. Cryst.* **2013,** *46*, 1513–1517.

40. Johansson, M.; Swart, M. *Intramolecular halogen–halogen bonds? Phys. Chem. Chem. Phys.* **2013**, *15*, 11543–11553.

41. Zhurova, E. A.; Tsirelson, V. G.; Stash, A. I.; Pinkerton, A. A. *Characterizing the oxygen-oxygen interaction in the dinitramide anion. J. Amer. Chem. Soc.* **2002**, *124*, 4574–4575.

42. Tsirelson, V. G.; Shishkina, A. V.; Stash, A. I.; Parsons, S. *The experimental and theoretical QTAIMC study of the atomic and molecular interactions in dinitrogen tetroxide*. *Acta Cryst. B* **2009**, *65*, 647–658.

43. Tsirelson, V. G.; Zou, P.-F.; Tang, T-H. Bader, R. F. W. *Topological definition of crystal structure: determination of the bonded interactions in solid molecular chlorine*. *Acta Cryst. A* **1995**, *51*, 143–153.

44. Vila, A.; Mosquera, R. A. *AIM study on the protonation of methyl oxiranes. J. Mol. Struct. THEOCHEM* **2001,** *546*, 63−72.

45. Matta, C. F.; Castillo, N.; Boyd, R. J. *Characterization of a Closed-Shell Fluorine−Fluorine Bonding Interaction in Aromatic Compounds on the Basis of the Electron Density. J. Phys. Chem. A* **2005**, 109, 3669−3681.

46. Shishkina, A. V.; Stash, A. I.; Civalleri, B.; Ellern, A.; Tsirelson V. G. *Electron-Density and Electrostatic-Potential Features of Orthorhombic Chlorine Trifluoride*. *Mendeleev Commun.*, **2010**, *20*, 161–164.

47. Palusiak, M.; Grabowski, S. J.*, Do intramolecular halogen bonds exist? Ab initio calculations and crystal structures' evidences. Struct. Chem.* **2007,** *18*, 859–864.

48. Schuster, P. *The Hydrogen Bond*, *Vol.1*, (Eds.: P. Schuster, G. Zundel, C. Sandorfy) North-Holland, Amsterdam, The Netherlands, **1976**, 683.

49. Hehre, W. J.; Radom, L.; von Schleyer P.; Pople, J. A. *Ab Initio Molecular Orbital Theory*, Wiley, New York, **1986**, 576.

50. Shields, Z.; Murray, J. S.; Politzer, P. *Directional tendencies of halogen and hydrogen bonds. Int. J. Quant. Chem.*, **2010,** *110*, 2823–2832

51. Politzer, P., Murray, J. S., Clark, T. *Halogen bonding: an electrostatically-driven highly directional noncovalent interaction. Phys. Chem. Chem. Phys.*, **2010**, *12*, 7748–7757.

52. Politzer, P., Riley, K. E., Bulat, F. A.; Murray, J. S. *Perspectives on halogen bonding and other σ-hole interactions: Lex parsimoniae (Occam's Razor). Comput. Theor. Chem.,* **2012**, *998*, 2–8.

53. Koch, W.; Holthausen, M. C. *A Chemist's Guide to Density Functional Theory*, VCH, Weinheim, **2001**, 293.

54. Perdew, J.P. ; Burke, K.; Ernzerhof, M.*, Generalized Gradient Approximation Made Simple. Phys. Rev. Lett.,* **1996**, *77*, 3865–3868

55. Perdew, J.P.; Wang Y. Accurate and simple analytic representation of the electron-gas correlation energy. Phys. Rev. B, **1992**, *45*, 13244–13249.

56. Granovsky, A. Firefly, version 7.1.G. 2009. http://classic.chem.msu.su/gran/firefly/index.html

57. Lu, T.; Chen, F. *Multiwfn: A multifunctional wavefunction analyzer. J. Comp. Chem.* **2012**, *33*, 580–592.

58. Hübschle, C. B.; Dittrich, B. *MoleCoolQt - a molecule viewer for charge-density research. J. Appl. Cryst.* **2011**, *44*, 238–257.

59. Hübschle, C. B.; Luger, P. *MolIso - a program for colour-mapped iso-surfaces. J. Appl. Cryst.* **2006**, *39*, 901–904.

60. Bader, R. F. W.; Stephens, M. E. *Spatial localization of the electronic pair and number distributions in molecules. J. Am. Chem. Soc.*, **1975**, *97*, 7391–7399.

61. Fradera, X.; Austen, M. A.; Bader, R. F. W. *The Lewis Model and Beyond. J. Phys. Chem. A* **1998**, 103, 304–314.

62. Keith, T. A. AIMALL, Version 12.06.03, **2012**, Professional. http://aim.tkgristmill.com

63. Martín Pendás, A.; Hernánde-Trujillo, J. *The Ehrenfest force field: topology and consequences for the definition of an atom in a molecule. J. Chem. Phys.* **2012**, 137, 134101–134110.

64. Novikov, S. S.; Shvehgeymer, G. A.; Sevost'yanova, V. V.; Shlyapochnikov, V. A. *Khimiya alifaticheskih i aciklicheskih soedineniy*. Moscow: «Khimiya» **1974** (In Russian)

65. Wang, Y.-G.; Matta, C.; Werstyuk N.H. *Comparison of Localization and Delocalization Indices Obtained with Hartree–Fock and Conventional Correlated Methods: Effect of Coulomb Correlation. J. Comput. Chem.,* **2003**, *24*, 1720–1729.

66. Martín Pendás, A.; Francisco, E.; Blanco, M. A. *Binding energies of first row diatomics in the light of the interacting quantum atoms approach J. Phys. Chem. A*, **2006**, *110*, 12864–12869.

67. Martín Pendás, A.; Blanco, M. A.; Francisco, E. *Francisco, Steric repulsions, rotation barriers, and stereoelectronic effects: a real space perspective. J. Comput. Chem.* **2009**, 15, 98–109.

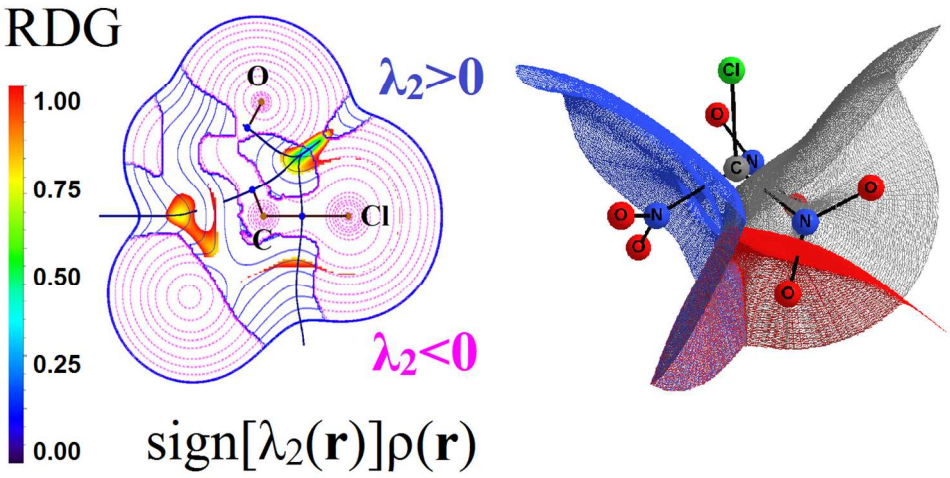

400x200mm (96 x 96 DPI)